2019

Sensor Placement for Damage Localization in Sensor Networks

Fereshteh Firouzi

Sensor Placement for Damage Localization in Sensor Networks

A thesis submitted in partial fulfillment of the requirements for the degree of Master of Science at Virginia Commonwealth University

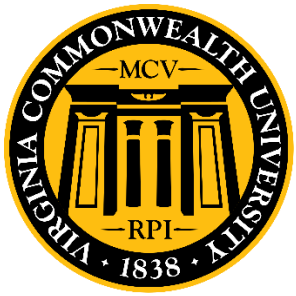

By

Fereshteh Firouzi

Adviser: Ruixin Niu, PhD,

Associate Professor, Department of Electrical and Computer Engineering

Virginia Commonwealth University

Richmond, Virginia

August, 2019

Acknowledgement

I would like to express my sincere gratitude to my adviser Dr. Ruixin Niu for his continuous encouragement through unique challenges faced by me as a graduate student. I have special thanks to Dr. Mulugeta Haile for providing me the opportunity to work on a fantastic topic and guiding me throughout my study. I would also like to thank the member of my thesis committee, Dr. Alen Docef, as well as Dr. Tao Sun for providing their helpful technical discussions.

Last but not least, I express my deepest gratitude to my family and dear husband for their continual support, prayers, and advice. Finally, I wish everyone good health and happiness.

Table of Contents

List of Tables

List of Figures

Abstract

The objective of this thesis is to formulate and solve the sensor placement problem for damage localization in a sensor network. A Bayesian estimation problem is formulated with the time-of-flight (ToF) measurements. In this model, ToF of lamb waves, which are generated and received by piezoelectric sensors, is the total time for each wave to be transmitted, reflected by the target, and received by the sensor. The ToF of the scattered lamb wave has characteristic information about the target location. By using the measurement model and prior information, the target location is estimated in a centralized sensor network with a Monte Carlo approach. Then we derive the Bayesian Fisher information matrix (B-FIM) and based on that posterior Cramer-Rao lower bound (PCRLB), which sets a limit on the mean squared error (MSE) of any Bayesian estimator. In addition, we develop an optimal sensor placement approach to achieve more accurate damage localization, which is based on minimizing the PCRLB. Simulation results show that the optimal sensor placement solutions lead to much lower estimation errors than some sub-optimal sensor placement solutions.

1 Chapter 1 Introduction

1.1 Background

In the past few years, the emergence of the networked multi-agent systems [1] is noticeable in different fields such as signal processing, automatic control, optimization, and communications. These systems can be used in numerous areas of sensor networks [2], robotic networks, unmanned aerial vehicles, and autonomous automobiles. Also, the network systems have been deployed in applications like defense, health, environment, and transportation. In all of these applications, damage[1] can occur over their operational life cycle. One of the important technologies to detect the damage is structural health monitoring (SHM) [3]. It monitors the structural performance and detects the fault at its early stage to avoid catastrophic failures [4] [5]. It provides information by combining sensor technology and algorithms.

One of the common sensor technologies for monitoring the structure health is piezoelectric sensors, due to the fact that they can be used as transmitter (Actuator) and receiver (Sensor) at the same time [6].

[1] Note: In this thesis, damage, fault, and target are used interchangeably.

Piezoelectric transducers generate lamb waves signals. The lamb-wave-based method is used as a SHM technique for fast damage detection in plate-like structures [7]. Lamb-waves spread over wide distances with low amplitude loss, hence increase the probability of large-area coverage. In addition, due to a high sensitivity, they can detect very small faults.

Sensor networks have been studied in research areas like sensing, detection, localization, and tracking of objects [8] [9]. They have a significant role in the performance of the SHM system, providing high coverage with small number of transducer elements [10]. It can be defined as an array of sensors schemed to get measurements from the environment.

We can evaluate the presence of damage by transmitting and receiving the reflected waves from sensors. This technique for damage detection utilizes distinct arrangements of piezoelectric transducers to activate and receive the lamb wave [11] [12]. One of these arrangements is pitch-catch method where lamb wave is transmitted by ultrasonic actuator and received by another ultrasonic sensor at a different position [13]. So, the damage localization method can be developed based on the range measurements to estimate the damage location. This algorithm can be applied using four different types of measurements such as, Time of Flight (ToF), Time Difference of Arrival (TDoA), Received Signal Strength indicator (RSSI), and Angle of Arrival (AoA).

The ToF method estimates distance between two nodes using time-based measurements. It is used here because of its high accuracy. The ToF of the scattered waves contains information about the damage location [14] [15] [16] [17]. Damage location is estimated by solving a set of nonlinear equations including the relation between damage location and ToF. These nonlinear equations were solved by using a nonlinear least squares Gauss–Newton optimization algorithm to estimate the damage location [16] [17].

In this thesis, the sizes of the actuators, sensors, and damage are not considered in damage localization. A maximum a posteriori probability (MAP) estimation method was proposed by Flynn *et al.* [10] which increases the damage localization probability. The likelihood function of the ToF measurements was presented in [18]. To estimate the damage location, we apply the Bayesian approach using the ToF measurements with consideration of the uncertainties from modeling and measurements in a centralized sensor network. The local sensor nodes transmit their measurements to a localization center which is based on a Monte-Carlo method to update the system state estimate.

Furthermore, sensor placement problem is investigated in this thesis. SHM systems gain the maximum probability of damage detection, if sensors are placed optimally [19]. Sensor placement plays an important role on the estimation accuracy of damage localization. In this thesis, the sensor placement problem is formulated as an optimization problem. Here the sensor positions need to be optimized to have a minimum error for damage localization [20]. For

optimization, we define a set of candidate sensor positions and select sensor positions which provide the most information in order to maximize estimation accuracy.

There are several existing criteria for sensor selection. Approaches for solving sensor placement for object estimation can be largely divided into two categories. The first criterion is based on information theoretic measures, such as entropy and mutual information. The Second one is based on posterior Cramer-Rao lower bound (PCRLB). The drawback of information theoretic measures is their high computational complexities which are exponential in the number of sensors and not applicable to a large sensor network, whereas the computational complexity of PCRLB is linear in the number of sensors. The PCRLB is a lower bound on the mean squared error (MSE) of any estimator of the random parameter, which indicates a performance limit and can be used as a criterion for optimal sensor placement. The PCRLB matrix is the inverse of Bayesian Fisher information matrix (B-FIM), which is obtained by summation of the expectation of the FIM and a term related to the prior information. So, the PCRLB [21] is used as a criterion for optimal sensor placement such that the minimum trace or the minimum determinant of the PCRLB matrix can be deemed as the maximum damage information gathered by the sensors.

In this thesis, we use a Monte Carlo method to compute the PCRLB for a nonlinear, Gaussian Bayesian estimation problem.

1.2 Main Contributions

In this section, we present our main contributions in the thesis:

- Apply the Bayesian estimation approach to the damage localization problem by utilizing the ToF of Lamb wave propagation and considering measurement uncertainty. We solve this estimation problem by using a Monte Carlo method.
- Derive the PCRLB as a sensor management criterion which is the inverse of the B-FIM. The B-FIM consists of contributions from both the measurement and the prior information.
- Implement optimized sensor placement by minimizing the PCRLB. The goal is maximizing the damage localization performance by designing an efficient algorithm for sensor placement.

1.3 Thesis Organization

The rest of the thesis is organized as follows. In Chapter 2, a Bayesian damage localization problem using TOF of scattered Lamb waves is formulated. Also, a Monte Carlo method for finding the posterior distribution of the damage position is presented. In Chapter 3, the Bayesian FIM and the PCRLB are mathematically derived. In Chapter 4, the PCRLB is applied for optimal sensor placement for damage estimation in sensor networks and an algorithm is proposed for solving the sensor placement problem. In Chapter 5, the numerical study for our model and simulation results are presented. Finally, conclusion and suggestions for future work are provided in Chapter 6.

2 Chapter 2 Bayesian Estimation

2.1 Bayesian Estimation Problems

The Bayesian approach is a statistical method that uses Bayes' theorem to obtain the posterior probability density function. It computes the estimate of the fault state using sensor measurements and prior information. In this thesis we use the Bayesian approach to find the fault location.

The general observation model to estimate the unknown fault is provided by the following measurement equation [22]:

$$\boldsymbol{z} = \mathrm{h}(\mathbf{x}, \mathbf{v}) \tag{2-1}$$

where h (.) is in general a nonlinear function, $\mathbf{x}$ is the state vector, and $\mathbf{v}$ is a white Gaussian measurement noise, which is assumed to be independent of $\mathbf{x}$. The unknown state, is modeled as a Gaussian distributed random variable with known mean and covariance [22].

2.2 Bayesian Approach for ToF-based Damage Localization

The Bayesian approach to estimate the damage location based on the ToF of lamb waves in sensor network, is presented in this section. To estimate the fault location, lamb waves will be sent from the actuators to the damage and then the reflected wave will be received by sensors. Pitch-catch method will be used for this sensor network, which means that the omnidirectional wave is sent to the surface of the plate and captured as a reflected wave returning at the reflected angle.

The ToF can be defined as the length of a path divided by the wave propagation speed.

We consider a plate with a centralized sensor network including multiple sensors and actuators. The ToF would be the total time for a lamb wave to be sent from an actuator to the damage, reflected by the damage, and received by a sensor.

We assume that the sensors, actuators, and damage are located in a 2-D plate. The ToF calculation for the lamb waves is illustrated in Figure 2-1.

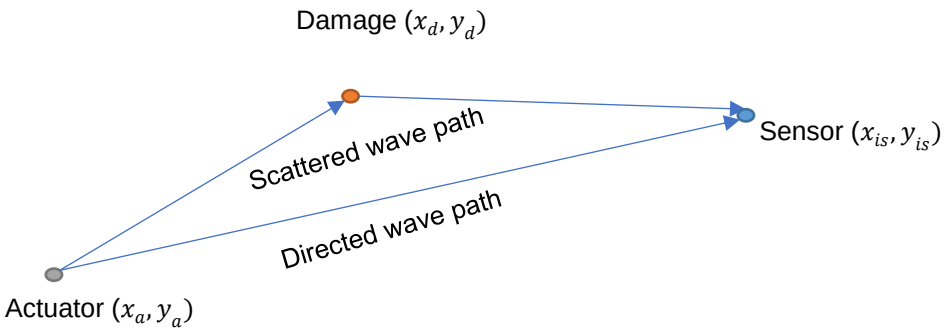

Figure 2-1. ToF model for the scattered Lamb wave in the ith actuator–sensor path.

The calculated ToF is shown in [14] as:

$$T_i^c(\boldsymbol{\theta}) = \frac{\sqrt{(x_d - x_a)^2 + (y_d - y_a)^2}}{V_g} + \frac{\sqrt{(x_d - x_{is})^2 + (y_d - y_{is})^2}}{V_g} \tag{2-2}$$

where (x_d,y_d) denotes damage location, (x_a,y_a) represents actuator location, and (x_{is},y_{is}) represents the ith sensor's location for $i = 1, 2, \dots, Np$. Therefore, there are totally Np different paths. The wave propagation speed (V_g) of the lamb waves is assumed to be a constant. The unknown parameters are (x_d,y_d), which are denoted by $\boldsymbol{\theta} = [\theta_1, \theta_2]^T = [x_d, y_d]^T$.

2.2.1 Measurement Model

Because of uncertainty, we model the measured ToF in the ith actuator–sensor path, T_i^m [14] as:

$$T_i^m = T_i^c\ (\boldsymbol{\theta}) + \varepsilon\ ,\ \varepsilon \sim \mathcal{N}(0,\ \sigma_\varepsilon^2) \tag{2-3}$$

in which ε is a white Gaussian measurement noise with zero mean and variance of σ_ε^2.

To calculate the posterior PDF, we need to find the likelihood function which is:

$$p(\boldsymbol{D}|\boldsymbol{\theta}) = \frac{1}{(2\pi\sigma_\varepsilon^2)^{Np/2}} * \exp\left[-\frac{1}{2\sigma_\varepsilon^2}\sum_{i=1}^{Np}(T_i^m - T_i^c\ (\boldsymbol{\theta}))^2\right] \tag{2-4}$$

where $\boldsymbol{D} = \left[\ T_1^m, T_2^m, \dots, T_{Np}^m\ \right]^{\mathrm{T}}$ is the measured ToF data.

Now the posterior PDF is defined as:

$$p(\boldsymbol{\theta}|\boldsymbol{D}) \propto p(\boldsymbol{D}|\boldsymbol{\theta}) p_\pi(\boldsymbol{\theta}) \tag{2-5}$$

where $p_\pi(\boldsymbol{\theta})$ is the prior PDF.

2.2.2 Centralized Sensor Network

As illustrated in Figure 2-2, in this centralized sensor network, sensors receive the raw ToF measurements and then will send them to the target localization center to estimate the target state.

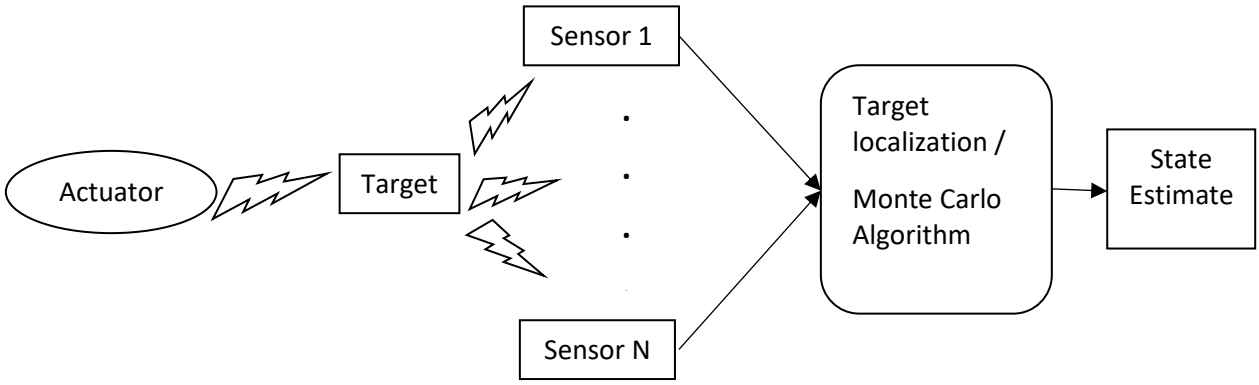

Figure 2-2. Centralized sensor network

2.3 A Monte Carlo Based Approach for Bayesian Estimation

2.3.1 Background

A Monte Carlo (MC) based approach is adopted in this thesis to calculate the probability distribution of the target state. This algorithm is based on sequential random sampling. We use this approach because the posterior probability density function (PDF) has no closed form. The MC based approaches can be used in different ways in statistics. One way is for numerical integration. In this case we have a nonlinear integral that is difficult to compute, and we can use this method to find the integration in a convenient way. Another usage is for optimization which alleviates the local minimum problem by allowing random exit from the local minimum and finds the global minimum. Also, Monte Carlo based approaches can be used for state estimation via important sampling [23] [24].

2.3.2 Monte Carlo Sampling

Using Monte Carlo sampling to estimate the posterior PDFs of unknown parameters, we generate a lot of random variables from the prior PDF. We sample normally distributed set of random variables with mean and covariance of the prior distribution.

We assume that unknown random variable $(\boldsymbol{\theta})$ is Gaussian distributed and find it from prior PDF $(p_\pi(\boldsymbol{\theta}))$ for N independent samples, called particles.

$\boldsymbol{\theta}_j \sim p_\pi(\boldsymbol{\theta}) \sim \mathcal{N}(\boldsymbol{\mu}, \boldsymbol{\Sigma}) \quad , \quad \mathrm{j} = 1, 2, \ldots, N$

The Monte-Carlo expectation would be as [24]:

$$E\{f(\boldsymbol{\theta})\} = \int f(\boldsymbol{\theta})\, p(\boldsymbol{\theta})\, d\boldsymbol{\theta} \approx \frac{1}{N}\sum_{j=1}^{N} f(\boldsymbol{\theta}_j) \tag{2-6}$$

where $p(\boldsymbol{\theta})$ is the PDF of $\boldsymbol{\theta}$ and $f(\boldsymbol{\theta})$ is an arbitrary function of $\boldsymbol{\theta}$.

This estimate approaches the true value if the number of samples goes to infinity. Due to the discrete nature of Monte Carlo sampling, it is difficult to find the PDF. Hence, with an approximation in terms of discrete distribution, we have:

$$p(\boldsymbol{\theta}) \approx \sum_{j=1}^{N} w_j \delta(\boldsymbol{\theta} - \boldsymbol{\theta}_j) \tag{2-7}$$

where w_j is proportional to the likelihood of each sample, namely

$$w_j \propto p(\boldsymbol{D}|\boldsymbol{\theta}_j)$$

2.3.3 Importance Sampling

We use importance sampling to generate samples from a proposal distribution [25]. Then importance sampling would be used to reweight the particles, hence we obtain an approximation of the true posterior distribution. We can use this technique as a variance reduction technique in the Monte Carlo method. In the importance sampling, some random samples with higher weight are more important than others. Hence, these more important samples are resampled more frequently, then it will lead to a reduction in estimator variance.

If we assume $p(\boldsymbol{\theta})$ and $\mathrm{g}(\boldsymbol{\theta})$ are desired and proposal density functions respectively, then $\mathrm{g}(\boldsymbol{\theta})$ can be chosen to have the minimum variance. w_j' is known as the importance weight.

$$w_j' \propto \frac{p(\boldsymbol{\theta})}{\mathrm{g}(\boldsymbol{\theta})} \tag{2-8}$$

where the normalized importance weights $\widetilde{w}_j's$ are given by:

$$\widetilde{w}_j\mathrm{'s} = \frac{w_j'}{\sum_{j=1}^{N} w_j'} \tag{2-9}$$

The estimated state can be approximated by:

$$\widehat{\boldsymbol{\theta}} \approx \sum_{j=1}^{N} \widetilde{w}_j\mathrm{'s}\ \boldsymbol{\theta}_j \tag{2-10}$$

2.4 Mean Squared Error (MSE)

The MSE gives us the information about the average squared difference between the estimated and true parameters. Hence lower MSE would be the desirable result.

The MSE matrix is defined as [22]:

$$\text{MSE} = E\left\{\left(\widehat{\boldsymbol{\theta}} - \boldsymbol{\theta}\right)\left(\widehat{\boldsymbol{\theta}} - \boldsymbol{\theta}\right)^{T}\right\} \tag{2-11}$$

where $\widehat{\boldsymbol{\theta}}$ and $\boldsymbol{\theta}$ are the estimated and true parameters respectively.

In the next section, we compare the obtained MSE with posterior Cramer-Rao lower band.

3 Chapter 3 Posterior Cramer-Rao Lower Bounds for Bayesian Estimation

3.1 Background

Cramer-Rao lower bound (CRLB) [22] is a lower bound on the variance of any unbiased estimator of a fixed parameter. It is derived by getting the inverse of Fisher information matrix, that is defined as an expectation of the negative second order derivative of the likelihood function.

Van Trees presented the posterior Cramer-Rao lower bound (PCRLB) [21] for estimators of random parameters. It provides a theoretic performance limit for a Bayesian estimator and creates a lower bound on the mean-squared error for any estimator of the random parameter. Here we want to obtain the optimal PCRLB for a sensor network in a centralized architecture.

3.2 Classical Cramer-Rao Lower Bounds

Van Trees showed that the MSE is bounded by the PCRLB [21] :

$$E\{(\hat{\boldsymbol{x}}(\boldsymbol{z})-\boldsymbol{x})(\hat{\boldsymbol{x}}(\boldsymbol{z})-\boldsymbol{x})^T\} \geq \boldsymbol{J}^{-1} \tag{3-1}$$

where state $\boldsymbol{x}$ is a random vector to be estimated and $\boldsymbol{z}$ is the observation. $\hat{\boldsymbol{x}}(\boldsymbol{z})$ is an estimator of $\boldsymbol{x}$ which is a function of $\boldsymbol{z}$. This inequality means that the MSE of any estimator cannot go below its PCRLB. The PCRLB can be used for both parameter estimation and state estimation.

where $\boldsymbol{J}$ is the posterior Fisher information matrix:

$$\boldsymbol{J} = E\left\{-\nabla_{\boldsymbol{x}}\nabla_{\boldsymbol{x}}{}^T \log p(\boldsymbol{x},\boldsymbol{z})\right\} \tag{3-2}$$

and the expectation is taken with respect to joint PDF $p(\boldsymbol{x},\boldsymbol{z})$. $\nabla_{\boldsymbol{x}}\nabla_{\boldsymbol{x}}{}^{T}$ is the second order derivative.

3.3 PCRLB for Nonlinear Damage Localization Problem

3.3.1 Fisher Information Matrix

In general, based on the Cramer-Rao lower bound theory, the mean squared error of any unbiased estimator should not be lower than the inverse of Fisher information matrix.

$$E\left\{\left[\widehat{\boldsymbol{\theta}}(\mathbf{D})-\boldsymbol{\theta}\right]^{2}\right\}\geq \boldsymbol{I}(\boldsymbol{\theta})^{-1} \tag{3-3}$$

We compute the Fisher information matrix $\boldsymbol{I}(\boldsymbol{\theta})$, which is obtained by taking the integral of the negative of the second order derivative of the log likelihood function [26].

$$\boldsymbol{I}(\theta)=-E\left\{\frac{\partial^{2} logp(\boldsymbol{D}|\boldsymbol{\theta})}{\partial\boldsymbol{\theta}^{2}}\right\}=E\left\{\left[\frac{\partial logp(\boldsymbol{D}|\boldsymbol{\theta})}{\partial\boldsymbol{\theta}}\right]^{2}\right\} \tag{3-4}$$

where $p(\boldsymbol{D}|\boldsymbol{\theta})$ is the likelihood function as we mentioned in (2-4).

The parameter vector is $\boldsymbol{\theta}=[\theta_1,\theta_2]^{T}$ which has two unknown parameters. Hence, we have a 2×2 Fisher information matrix [26].

$$\boldsymbol{I}(\boldsymbol{\theta})=\begin{bmatrix} E\left\{\left[\frac{\partial logp(\boldsymbol{D}|\boldsymbol{\theta})}{\partial\theta_1}\right]^{2}\right\} & E\left\{\frac{\partial logp(\boldsymbol{D}|\boldsymbol{\theta})}{\partial\theta_1}\frac{\partial logp(\boldsymbol{D}|\boldsymbol{\theta})}{\partial\theta_2}\right\} \\ E\left\{\frac{\partial logp(\boldsymbol{D}|\boldsymbol{\theta})}{\partial\theta_1}\frac{\partial logp(\boldsymbol{D}|\boldsymbol{\theta})}{\partial\theta_2}\right\} & E\left\{\left[\frac{\partial logp(\boldsymbol{D}|\boldsymbol{\theta})}{\partial\theta_2}\right]^{2}\right\} \end{bmatrix} \tag{3-5}$$

The matrix is symmetric and it is positive definite.

From (2-4), the log-likelihood function can be derived as:

$$logp(\boldsymbol{D}|\boldsymbol{\theta}) = \log\frac{1}{(2\pi\sigma_\varepsilon^2)^{Np/2}} - \frac{1}{2\sigma_\varepsilon^2}\sum_{i=1}^{Np}(T_i^m - T_i^c(\boldsymbol{\theta}))^2) \tag{3-6}$$

Since $log\frac{1}{(2\pi\sigma_\varepsilon^2)^{Np/2}}$ is not dependent on $\boldsymbol{\theta}$, so its derivative with respect to $\boldsymbol{\theta}$ would be zero.

The derivative of $logp(\boldsymbol{D}|\boldsymbol{\theta})$ with respect to θ_1 is:

$$\frac{\partial logp(\boldsymbol{D}|\boldsymbol{\theta})}{\partial\theta_1} = \frac{1}{\sigma_\varepsilon^2}\sum_{i=1}^{Np}(T_i^m - T_i^c(\boldsymbol{\theta}))\left(\frac{\partial T_i^c(\boldsymbol{\theta})}{\partial\theta_1}\right) \tag{3-7}$$

where $\frac{\partial T_i^c(\boldsymbol{\theta})}{\partial\theta_1}$ is:

$$\begin{aligned}\left(\frac{\partial T_i^c(\boldsymbol{\theta})}{\partial\theta_1}\right) &= \frac{(\theta_1 - x_a)[(\theta_1 - x_a)^2 + (\theta_2 - y_a)^2]^{-1/2}}{V_g} \\ &+ \frac{(\theta_1 - x_{is})[(\theta_1 - x_{is})^2 + (\theta_2 - y_{is})^2]^{-1/2}}{V_g}\end{aligned} \tag{3-8}$$

Similarly, the derivative of $logp(\boldsymbol{D}|\boldsymbol{\theta})$ with respect to θ_2 is:

$$\frac{\partial logp(\boldsymbol{D}|\boldsymbol{\theta})}{\partial\theta_2} = \frac{1}{\sigma_\varepsilon^2}\sum_{i=1}^{Np}(T_i^m - T_i^c(\boldsymbol{\theta}))\left(\frac{\partial T_i^c(\boldsymbol{\theta})}{\partial\theta_2}\right) \tag{3-9}$$

where $\frac{\partial T_i^c(\boldsymbol{\theta})}{\partial\theta_2}$ is:

$$\begin{aligned}\left(\frac{\partial T_i^c(\boldsymbol{\theta})}{\partial\theta_2}\right) &= \frac{(\theta_2 - y_a)[(\theta_1 - x_a)^2 + (\theta_2 - y_a)^2]^{-1/2}}{V_g} \\ &+ \frac{(\theta_2 - y_{is})[(\theta_1 - x_{is})^2 + (\theta_2 - y_{is})^2]^{-1/2}}{V_g}\end{aligned} \tag{3-10}$$

To solve each term of the FIM, we calculate the expectation of these derived derivatives.

$$E\left\{\left[\frac{\partial logp(\boldsymbol{D}|\boldsymbol{\theta})}{\partial \theta_1}\right]^2\right\} = \frac{1}{\sigma_\varepsilon^2}\sum_{i=1}^{Np}\left(\frac{\partial T_i^c(\boldsymbol{\theta})}{\partial \theta_1}\right)^2 \tag{3-11}$$

$$E\left\{\left[\frac{\partial logp(\boldsymbol{D}|\boldsymbol{\theta})}{\partial \theta_2}\right]^2\right\} = \frac{1}{\sigma_\varepsilon^2}\sum_{i=1}^{Np}\left(\frac{\partial T_i^c(\boldsymbol{\theta})}{\partial \theta_2}\right)^2 \tag{3-12}$$

$$E\left\{\frac{\partial logp(\boldsymbol{D}|\boldsymbol{\theta})}{\partial \theta_1}\ \frac{\partial logp(\boldsymbol{D}|\boldsymbol{\theta})}{\partial \theta_2}\right\} = \frac{1}{\sigma_\varepsilon^2}\sum_{i=1}^{Np}\left(\frac{\partial T_i^c(\boldsymbol{\theta})}{\partial \theta_1}\right)\left(\frac{\partial T_i^c(\boldsymbol{\theta})}{\partial \theta_2}\right) \tag{3-13}$$

So, the FIM would be:

$$\boldsymbol{I}(\boldsymbol{\theta}) = \frac{1}{\sigma_\varepsilon^2}\begin{bmatrix} \sum_{i=1}^{Np}\left(\frac{\partial T_i^c(\boldsymbol{\theta})}{\partial \theta_1}\right)^2 & \sum_{i=1}^{Np}\left(\frac{\partial T_i^c(\boldsymbol{\theta})}{\partial \theta_1}\right)\left(\frac{\partial T_i^c(\boldsymbol{\theta})}{\partial \theta_2}\right) \\ \sum_{i=1}^{Np}\left(\frac{\partial T_i^c(\boldsymbol{\theta})}{\partial \theta_1}\right)\left(\frac{\partial T_i^c(\boldsymbol{\theta})}{\partial \theta_2}\right) & \sum_{i=1}^{Np}\left(\frac{\partial T_i^c(\boldsymbol{\theta})}{\partial \theta_2}\right)^2 \end{bmatrix} \tag{3-14}$$

3.3.2 Bayesian Fisher Information Matrix

Now, after calculating the FIM, we present the B-FIM as:

$$\text{B-FIM} = \int \boldsymbol{I}(\boldsymbol{\theta}) p_\pi(\boldsymbol{\theta})\, d\boldsymbol{\theta} + E_{p_\pi}\{-\nabla_{\boldsymbol{\theta}}\nabla_{\boldsymbol{\theta}}^T log\, p_\pi(\boldsymbol{\theta})\} = \boldsymbol{I}_D + \boldsymbol{I}_P \tag{3-15}$$

B-FIM consists of two parts. The first part is the integral of classical-FIM with respect to the prior distribution $p_\pi(\boldsymbol{\theta})$ and the second part is related to the prior information.

3.3.2.1 Integral of Classical-FIM

To solve the first part ($\boldsymbol{I}_D$), because of the nonlinearity of Fisher information matrix elements, it is difficult to solve the double integral. We use a set of random samples (particles) and apply a Monte-Carlo method to calculate the integral.

We can consider prior PDF as a summation of N_{pc} number of particles:

$$p_\pi(\boldsymbol{\theta}) \approx \frac{1}{N_{pc}}\sum_{j=1}^{N_{pc}} \delta(\boldsymbol{\theta}-\boldsymbol{\theta}^{(j)}) \qquad \& \qquad \boldsymbol{\theta}^{(j)} = [{x_d}^{(j)}, {y_d}^{(j)}]^T \sim p_\pi(\boldsymbol{\theta}) \tag{3-16}$$

$$\begin{aligned} \boldsymbol{I}_D &= \int I(\boldsymbol{\theta}) p_\pi(\boldsymbol{\theta})\, d\boldsymbol{\theta} \\ &= \int \boldsymbol{I}(\boldsymbol{\theta}) \frac{1}{N_{pc}} \sum_{j=1}^{N_{pc}} \delta(\boldsymbol{\theta}-\boldsymbol{\theta}^{(j)})\, d\boldsymbol{\theta} \\ &= \frac{1}{N_{pc}} \sum_{j=1}^{N_{pc}} \int \delta\left(\boldsymbol{\theta}-\boldsymbol{\theta}^{(j)}\right)\, \boldsymbol{I}(\boldsymbol{\theta}) d\boldsymbol{\theta} \end{aligned} \tag{3-17}$$

Based on the [27] , using the Dirac (impulse) delta function defined by:

$$\delta(\boldsymbol{x}) = 0 \quad \forall\, \boldsymbol{x} \neq 0 \tag{3-18}$$

and

$$\int_{-\infty}^{\infty} \delta(\boldsymbol{x})\, d\boldsymbol{x} = 1 \tag{3-19}$$

We have $\int \delta\left(\boldsymbol{\theta}-\boldsymbol{\theta}^{(j)}\right) d\boldsymbol{\theta} = 1$, then the first part of equation would be:

$$\boldsymbol{I}_D = \int \boldsymbol{I}(\boldsymbol{\theta}) p_\pi(\boldsymbol{\theta})\, d\boldsymbol{\theta} = \frac{1}{N_{pc}}\sum_{j=1}^{N_{pc}} \boldsymbol{I}(\boldsymbol{\theta}^{(j)}) \tag{3-20}$$

The above satisfies the normalization property of a PDF in that it integrates to unity. Hence by summing FIM matrices evaluated at N_{pc} number of particles, we have an approximation of the integral.

3.3.2.2 Prior-FIM

To solve the second part ($\boldsymbol{I}_P$), we calculate the expectation with respect to the prior distribution. The probability density function (PDF) of a Gaussian (normal) random variable, $x \sim \mathcal{N}(\mu, \sigma^2)$, is:

$$p(x) = \mathcal{N}(x; \mu, \sigma^2) \triangleq \frac{1}{\sqrt{2\pi}\,\sigma} e^{\frac{(x-\mu)^2}{2\sigma^2}} \tag{3-21}$$

We assume that the prior distribution follows a Gaussian distribution.

$$p_\pi(\boldsymbol{\theta}) \sim \mathcal{N}(\boldsymbol{\mu}, \boldsymbol{\Sigma})$$

where $\boldsymbol{\mu} = [\mu_1, \mu_2]^T$ and $\boldsymbol{\Sigma}$= diag (σ^2, σ^2) are the mean and covariance matrix of the prior distribution.

Because we have two unknown random variables, which are independent, so the probability density function is multiplication of PDFs of the two random variables.

$$p_\pi(\boldsymbol{\theta}) = \frac{1}{2\pi\sigma^2} \exp\left\{-\frac{1}{2\sigma^2}[(\theta_1 - \mu_1)^2 + (\theta_2 - \mu_2)^2]\right\} \tag{3-22}$$

With 3-22) $\boldsymbol{I}_P$ becomes:

$$\boldsymbol{I}_P = \begin{bmatrix} E\left\{\frac{\partial log p_\pi(\boldsymbol{\theta})}{\partial \theta_1}\right\}^2 & E\left\{\frac{\partial log p_\pi(\boldsymbol{\theta})}{\partial \theta_1}\frac{\partial log p_\pi(\boldsymbol{\theta})}{\partial \theta_2}\right\} \\ E\left\{\frac{\partial log p_\pi(\boldsymbol{\theta})}{\partial \theta_1}\frac{\partial log p_\pi(\boldsymbol{\theta})}{\partial \theta_2}\right\} & E\left\{\frac{\partial log p_\pi(\boldsymbol{\theta})}{\partial \theta_2}\right\}^2 \end{bmatrix} \quad (3\text{-}23)$$

Taking the logarithm on both sides of (3-22), we have:

$$log p_\pi(\boldsymbol{\theta}) = \log\frac{1}{2\pi\sigma^2} - \frac{1}{2\sigma^2}[(\theta_1 - \mu_1)^2 + (\theta_2 - \mu_2)^2] \quad (3\text{-}24)$$

By taking derivative of $log p_\pi(\boldsymbol{\theta})$ with respect to the random variable (θ_1, θ_2), only functions of (θ_1, θ_2) are considered for derivation and the rest becomes zero.

$$\frac{\partial log p_\pi(\boldsymbol{\theta})}{\partial \theta_1} = -\frac{1}{\sigma^2}(\theta_1 - \mu_1) \quad (3\text{-}25)$$

$$\frac{\partial log p_\pi(\boldsymbol{\theta})}{\partial \theta_2} = -\frac{1}{\sigma^2}(\theta_2 - \mu_2) \quad (3\text{-}26)$$

By taking the expectation of these derivatives, we have:

$$E\left\{\frac{\partial log p_\pi(\boldsymbol{\theta})}{\partial \theta_1}\right\}^2 = \frac{1}{\sigma^2} \quad (3\text{-}27)$$

$$E\left\{\frac{\partial log p_\pi(\boldsymbol{\theta})}{\partial \theta_2}\right\}^2 = \frac{1}{\sigma^2} \quad (3\text{-}28)$$

Because these two unknown parameters are independent, hence:

$$E\left\{\frac{\partial log p_\pi(\boldsymbol{\theta})}{\partial \theta_1}\frac{\partial log p_\pi(\boldsymbol{\theta})}{\partial \theta_2}\right\} = 0 \quad (3\text{-}29)$$

So,

$$\boldsymbol{I}_P = \begin{bmatrix} \frac{1}{\sigma^2} & 0 \\ 0 & \frac{1}{\sigma^2} \end{bmatrix} \tag{3-30}$$

By summing both parts, the B-FIM is determined as:

$$\text{B-FIM} = \frac{1}{N_{pc}} \sum_{j=1}^{N_{pc}} \boldsymbol{I}(\boldsymbol{\theta}^{(j)}) + \begin{bmatrix} \frac{1}{\sigma^2} & 0 \\ 0 & \frac{1}{\sigma^2} \end{bmatrix} \tag{3-31}$$

3.3.3 Bayesian Cramer-Rao Lower Bound

By finding B-FIM in the previous section, the PCRLB matrix is simply its inverse:

$$\text{PCRLB} = (\text{B-FIM})^{-1}$$

To improve the estimation results, we can use the PCRLB as a sensor management criterion for the optimal sensor placement. In the next section, we will show how we use the minimum PCRLB criterion for sensor placement. After finding both the MSE and PCRLB, we can compare them to show that the PCRLB indeed gives a lower bound on the MSE that an estimator can achieve. In Chapter 5, the results for this inequality will be shown.

4 Chapter 4 Sensor Placement for Damage Localization

4.1 Sensor Management Criteria

The objective of the sensor placement problem is to determine sensor locations that minimize the estimation error. The sensor positions are the parameters that we want to optimize. Therefore, the estimated target location based on the optimization will be more accurate.

Approaches to solve the sensor management for target localization/tracking are mostly based on two criteria. The first one is based on the PCRLB [28] [29] and the second one is based on information theoretic measures, such as entropy, mutual information, etc. [30] [31, 32]. However, information theoretic measures are computationally intensive, particularly for a large number of sensors, because it is exponential in the number of sensors, whereas PCRLB is linear in the number of sensors [33]. Hence, we propose a posterior Cramer Rao lower bound based approach to optimize the positions of sensors.

4.2 Sensor Placement Based on PCRLB

In this problem, the minimum trace or determinant of the PCRLB, can be defined as the maximum measurement information of the target location received by the sensors. Our goal is, to determine the optimal sensor locations based on the prior information of the target position.

To solve the optimal sensor placement, we

1. Use the derived Fisher information in the past section to evaluate the estimation accuracy.
2. Design an algorithm to find the optimum sensor locations by minimizing the trace of the PCRLB.

4.2.1 Algorithm for Optimal Sensor Placement

We assume a 2-D plate with area of A × B. The plate is discretized in to M cells (grid points) and each cell has unit area. Sensors are placed in these cells. We have N sensors with K possible locations, and the sensors should be placed such that the minimum cost (trace of PCRLB) will be obtained. Having N sensors and K possible locations, the combination of $\binom{K}{N}$ would be the search space for sensor placement, which is infeasible to compute if we assume lots of possible locations for sensors [34].

Hence to find the optimum sensor locations, we use a person-by-person algorithm which can be used for large optimization problem [35]. This algorithm is guaranteed to find a locally optimal solution after its convergence. It optimizes one sensor's location at each step. The algorithm will end by achieving minimum trace of PCRLB after the iterations end [36].

Because our sensor placement algorithm is based on the Bayesian CRLB, then the B-FIM should be used which is obtained in (3-31):

$$\text{B-FIM} = \bar{\boldsymbol{I}}(\boldsymbol{\theta}) = \boldsymbol{I}_D + \boldsymbol{I}_P$$

$$\text{PCRLB} = [\bar{\boldsymbol{I}}(\boldsymbol{\theta})]^{-1}$$

The minimum trace of PCRLB would be the minimum cost.

Definition 1: A point $\boldsymbol{p}^*$ is an optimum sensor location if

$$\boldsymbol{p}^* = \arg\min(J_T(\boldsymbol{p})) \qquad \text{where} \quad J_T(\boldsymbol{p}) = \text{trace (PCRLB)}$$

In this algorithm, we initialize sensor positions in M by M grid. Then we assume that N sensors follow a uniform distribution within a plate:

$$a \leq, p_{ixs} \leq b \; ; a \leq p_{iys} \leq b \qquad , \qquad i = 1, 2, \dots, N$$

(a, b) is the range specified for sensor locations in the plate.

To perform optimization,

1. First, we need to initialize the sensor's location. We assume random value for the sensor's location within the specified range of a plate.
2. We suppose Sensor 1 location is a variable and other $(N - 1)$ sensors are fixed. Among all the possible grid locations for Sensor 1, the location that has the minimum trace of PCRLB will be selected as the optimum position.
3. After finding the optimum location for Sensor 1, we do the same for the next sensor. It means that Sensor 2's location is variable now and Sensor 1, Sensor 3, ..., Sensor N are fixed. Again, the best location for Sensor 2 will be found with the minimum trace of PCRLB.
4. In this way, in each loop one sensor would be variable and the rest are fixed to find the optimum sensor position for the minimum PCRLB. This loop would be repeated until the result (trace of PCRLB) converges and improvement is really small. So, the result gives us the optimum locations by achieving minimum trace of PCRLB.

5 Chapter 5 Simulation Results

5.1 Sensor Geometry

We assume a square plate for the model. The size of the plate is 300 mm × 300 mm. Four sensors, one actuator, and the damage are on this plate. The origin of the coordinate system is set at the center of the plate. The table and figure below show the plate layout. All the measurements are in mm [14].

Table 5-1. Coordinates of the actuator, sensors and damage on the plate

	Actuator	Sensor 1	Sensor 2	Sensor 3	Sensor 4	Damage
Coordinates(mm)	$\begin{pmatrix}0\\0\end{pmatrix}$	$\begin{pmatrix}-90\\-90\end{pmatrix}$	$\begin{pmatrix}-90\\90\end{pmatrix}$	$\begin{pmatrix}90\\-90\end{pmatrix}$	$\begin{pmatrix}90\\90\end{pmatrix}$	$\begin{pmatrix}40\\20\end{pmatrix}$

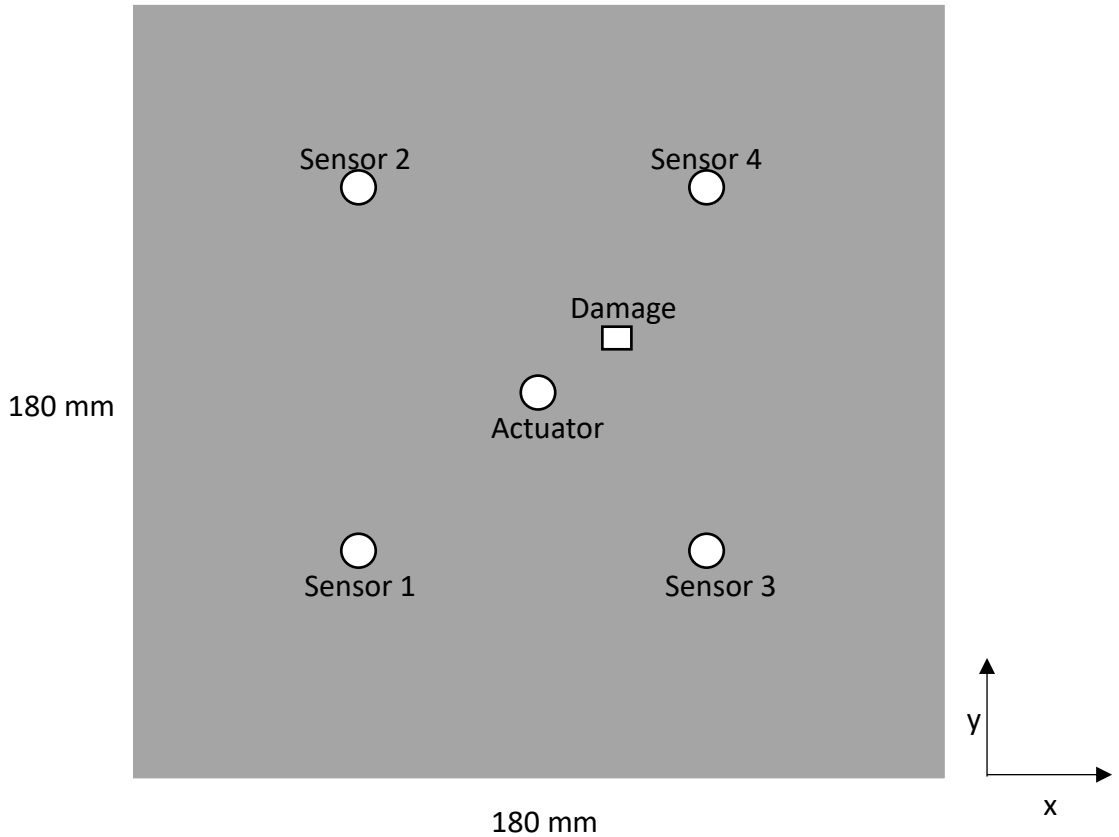

Figure 5-1. Layout of a plate with an actuator, sensors, and damage

We assume that, the wave propagation speed is V_g =1500 × 10^3 mm/sec.

Also, measurement noise ε, which was defined in (2-3), is Gaussian with σ_ε^2 =10^{-12}.

To estimate the posterior distribution, we use 10,000 Monte-Carlo runs. The prior PDF of the target state is assumed to be Gaussian with mean $\boldsymbol{\mu} = \binom{40}{20}$, and covariance matrix $\boldsymbol{\Sigma} = \begin{bmatrix} {\sigma_x}^2 & 0 \\ 0 & {\sigma_y}^2 \end{bmatrix}$

Standard deviations of $\sigma_x = 5$, $\sigma_y = 5$ would be assumed for the prior information.

The updated estimate in (2-10) is:

$$\widehat{\boldsymbol{\theta}} \approx \sum_{j=1}^{N} \tilde{w}_j\text{'s } \boldsymbol{\theta}_j$$

The equation is the weighted sum of the particles with $N = 10^5$ particles. After finding the updated estimate, the MSE will be achieved as well.

5.2 Damage Location Estimation

Estimation for damage localization is simulated by Monte-Carlo sampling in MATLAB. Figures 5-2 and 5-3 show the minimum mean squared error (MMSE) estimates (the mean of posterior PDF) of x and y coordinates of location of damage over 10,000 Monte Carlo runs.

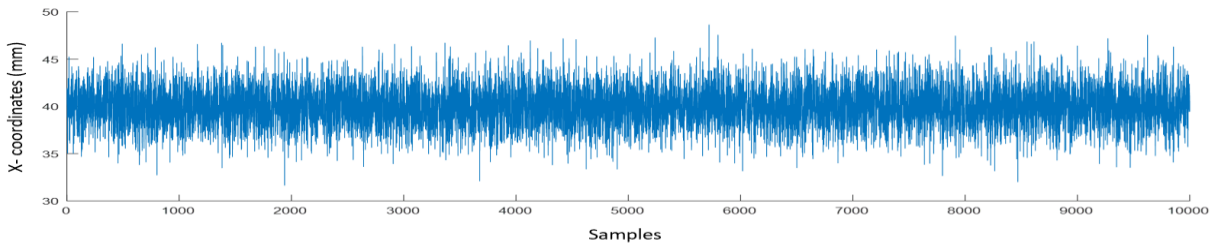

Figure 5-2. MC samples for MMSE estimates of X-coordinate of damage location

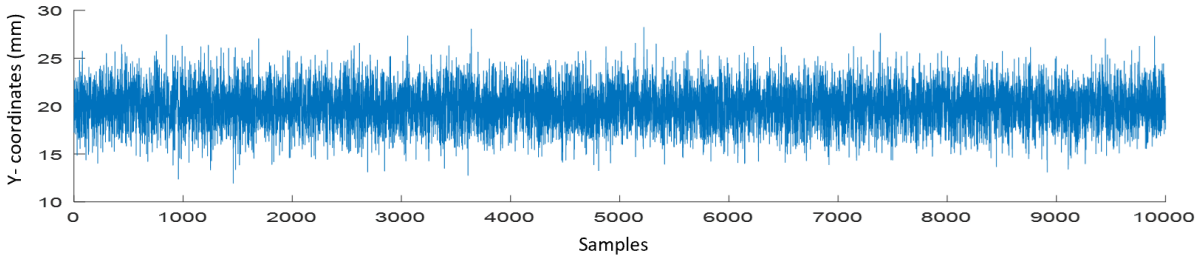

Figure 5-3. MC samples for MMSE estimates of Y-coordinate of damage location

The histograms for the two parameters are illustrated in Figures 5-4 and 5-5 respectively. Normal distributions are employed to fit the histograms.

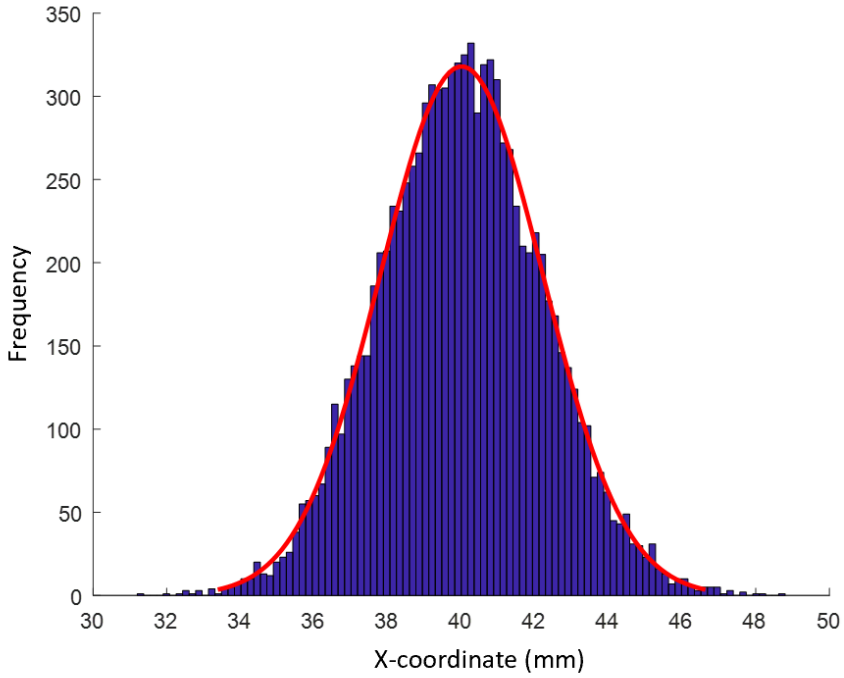

Figure 5-4. Histograms of MC samples for the mean of posterior PDF of X-coordinate

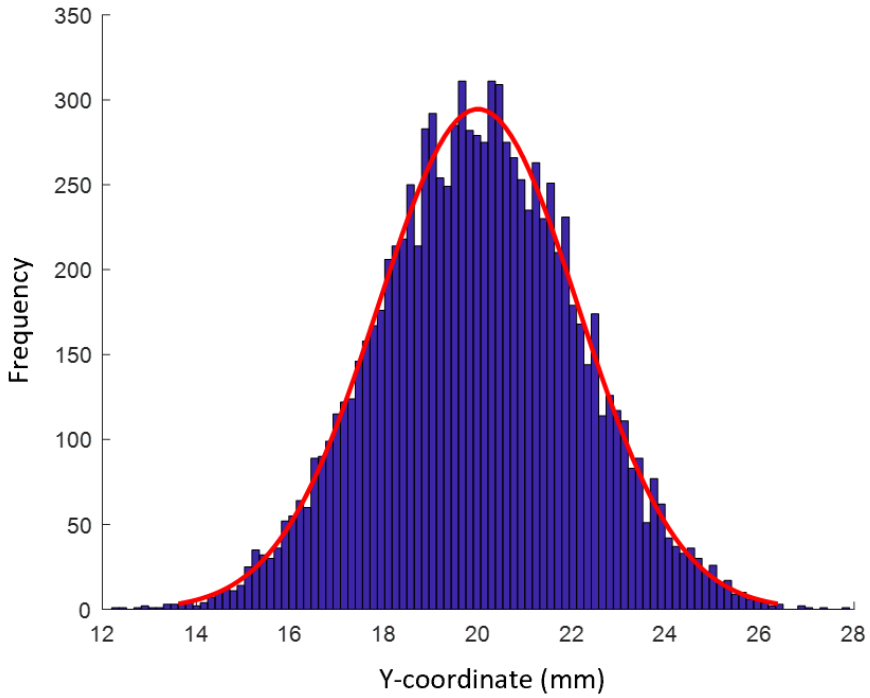

Figure 5-5. Histograms of MC samples for the mean of posterior PDF of Y-coordinate

Figures 5-6 and 5-7 display the joint prior and posterior PDF of the x–y coordinates of the location of damage in 3D. In comparison, we can see that the variance of the posterior information is reduced.

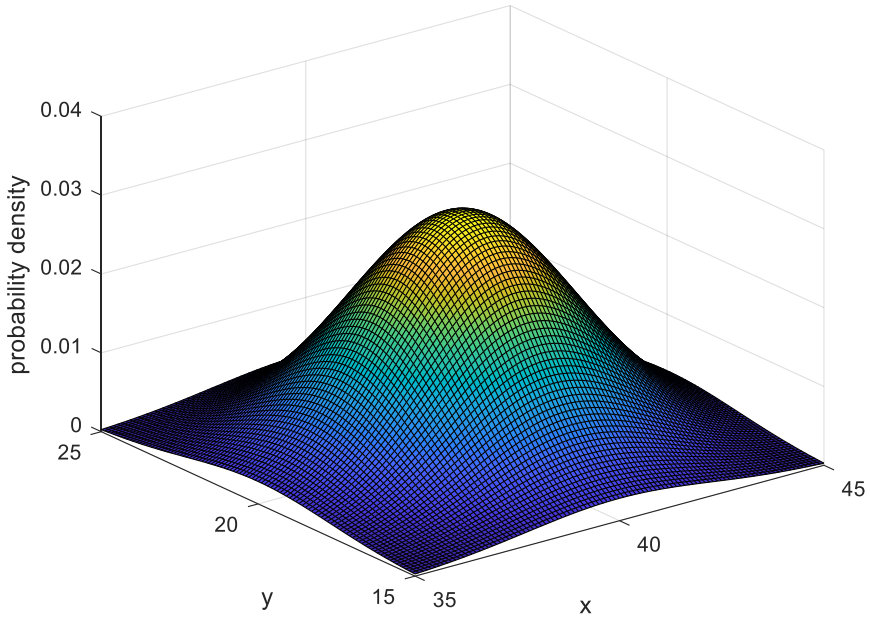

Figure 5-6. Joint prior PDF of x-y coordinates of damage location

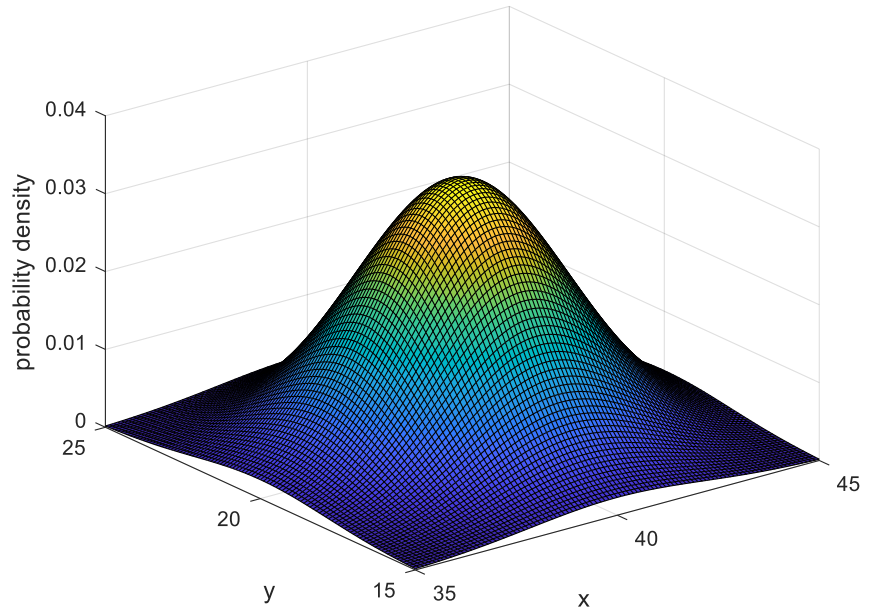

Figure 5-7. Joint posterior PDF of x-y coordinates of damage location

The contour of posterior PDF is shown in Figure 5-8.

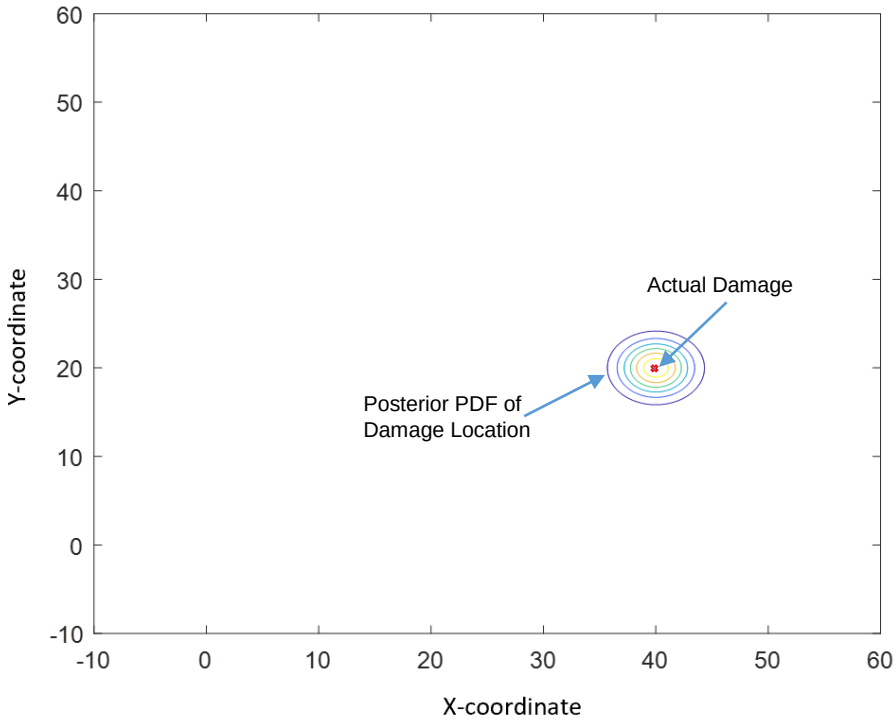

Figure 5-8. Joint posterior PDF in 2D contour

5.3 MSE vs. PCRLB

In this section, we compare the MSE with the corresponding Bayesian CRLB. According to the Cramer-Rao lower bound, the MSE corresponding to the estimator of a parameter should be larger than or equal to its lower bound. So the MSE is bounded from below as follows:

$$\mathrm{E}\left\{\left[\widehat{\boldsymbol{\theta}}(\mathbf{D})-\boldsymbol{\theta}\right]^{2}\right\} \geq \boldsymbol{I}^{-1} \quad , \ \boldsymbol{I}^{-1} = \text{ PCRLB}$$

These tables display MSE and PCRLB values for x and y coordinates of the damage location. This comparison has been evaluated for different measurement noises.

Table 5-2. MSE and PCRLB for $\sigma_\varepsilon^2 = 10^{-15}$

$\sigma_\varepsilon^2 = 10^{-15}$	$\theta_1(x_d)$	$\theta_2(y_d)$
PCRLB	0.00049	0.00096
MSE	0.00071	0.0014

Table 5-3. MSE and PCRLB for $\sigma_\varepsilon^2 = 10^{-14}$

$\sigma_\varepsilon^2 = 10^{-14}$	$\theta_1(x_d)$	$\theta_2(y_d)$
PCRLB	0.0049	0.0096
MSE	0.0051	0.0140

Table 5-4. MSE and PCRLB for $\sigma_\varepsilon^2 = 10^{-13}$

$\sigma_\varepsilon^2 = 10^{-13}$	$\theta_1(x_d)$	$\theta_2(y_d)$
PCRLB	0.0485	0.09
MSE	0.0509	0.099

Table 5-5. MSE and PCRLB for $\sigma_\varepsilon^2 = 10^{-12}$

$\sigma_\varepsilon^2 = 10^{-12}$	$\theta_1(x_d)$	$\theta_2(y_d)$
PCRLB	0.45	0.83
MSE	0.4838	0.8758

Table 5-6. MSE and PCRLB for $\sigma_\varepsilon^2 = 10^{-11}$

$\sigma_\varepsilon^2 = 10^{-11}$	$\theta_1(x_d)$	$\theta_2(y_d)$
PCRLB	2.79	4.2
MSE	2.96	4.4

As we see, both the MSE and PCRLB would increase, as the noise level increases. For all the different noise levels, the MSE is larger than the PCRLB, as expected.

The graphs of this comparison are shown in Figures 5-9 and 5-10. As we can see, as noise level increases, the estimation error increases as well.

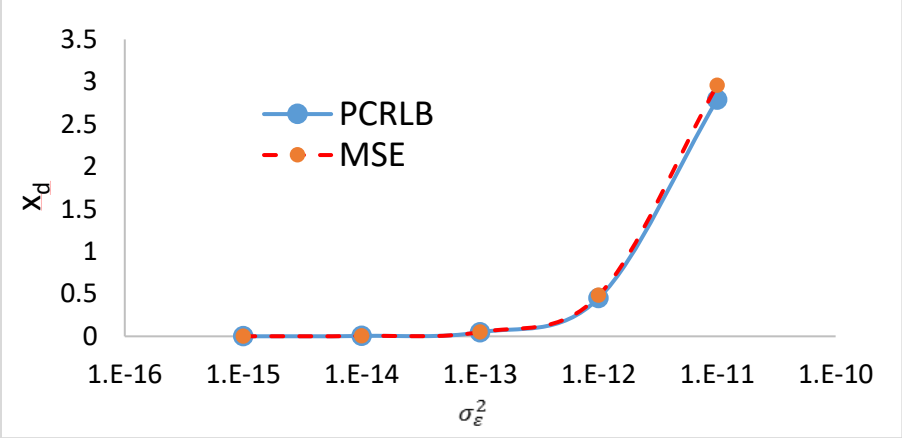

Figure 5-9. MSE and PCRLB for x_d with increasing noise variance

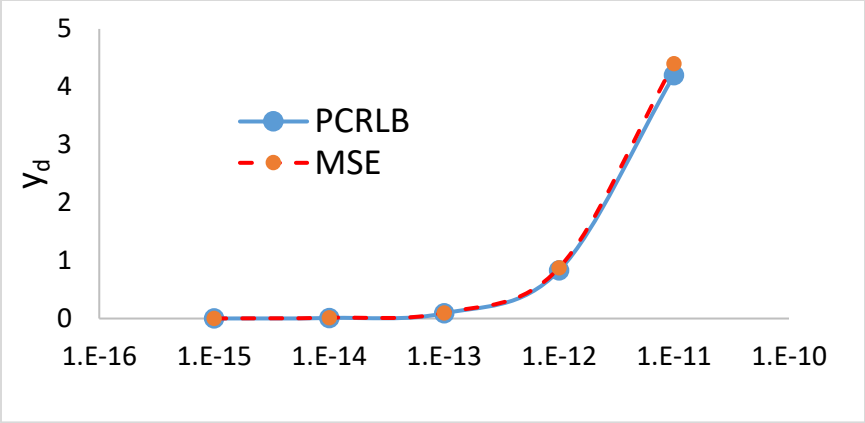

Figure 5-10. MSE and PCRLB for y_d with increasing noise variance

5.4 Sensor Placement Geometry

In the sensor placement, we suppose our sensors are randomly distributed. In this thesis, the minimum number of sensors (3 sensors) are deployed in the 180×180 field to find the optimum estimation. All these 3 sensors are placed in the specified range of:

$\boldsymbol{p}_{s1}$: $-90 \leq p_{1xs} \leq 90$; $-90 \leq p_{1ys} \leq 90$

$\boldsymbol{p}_{s2}$: $-90 \leq p_{2xs} \leq 90$; $-90 \leq p_{2ys} \leq 90$

$\boldsymbol{p}_{s3}$: $-90 \leq p_{3xs} \leq 90$; $-90 \leq p_{3ys} \leq 90$

Implement the sensor placement algorithm:

- $\boldsymbol{p}_{s1}$ is a variable between [-90, 90] and $\boldsymbol{p}_{s2}$ & $\boldsymbol{p}_{s3}$ are fixed at their initial values. Among all the possible grid locations for Sensor 1, the location that has the minimum trace of PCRLB will be selected as the best position.

  $M = set\ of\ all\ Sensor\ 1\ locations$
  $\boldsymbol{p}_{s2}$ & $\boldsymbol{p}_{s3} = constant\ (initial\ value)$
  $Tr\_PCRLB = \infty$
  $for\ esch\ sensor\ location\ j \in M$

  $compute\ the\ trace\ of\ PCRLB$:
  $Tr\_PCRLB(j)$ corresponding to sensor locations j

  $if\ Tr\_PCRLB > Tr\_PCRLB(j)$
  $Tr\_PCRLB = Tr\_PCRLB(j)$
  $best\_\boldsymbol{p}_{s1} = \boldsymbol{p}_{s1}(j)$

- After finding the $best\_\boldsymbol{p}_{s1}$, we do the same for $\boldsymbol{p}_{s2}$ & $\boldsymbol{p}_{s3}$ to find the $best\_\boldsymbol{p}_{s2}$ and $best\_\boldsymbol{p}_{s3}$.

- Repeat this algorithm until the improvement is really small.

5.5 Optimal Sensor Placement

In this section, we design sensor placement such that the lowest trace of the posterior CRLB is achieved. We find optimal sensor placement for different locations of damage and actuator. In this way we can observe the effect of actuator locations on the sensor placement solutions.

Example 1. Mean of the Damage location $= \binom{40}{20}$, Actuator $= \binom{0}{0}$

The optimum sensor placement with actuator placed on the origin is shown in Figure 5-11.

$\boldsymbol{p}_{s1} = \binom{38}{18}$, $\boldsymbol{p}_{s2} = \binom{56}{-90}$, $\boldsymbol{p}_{s3} = \binom{-18}{90}$

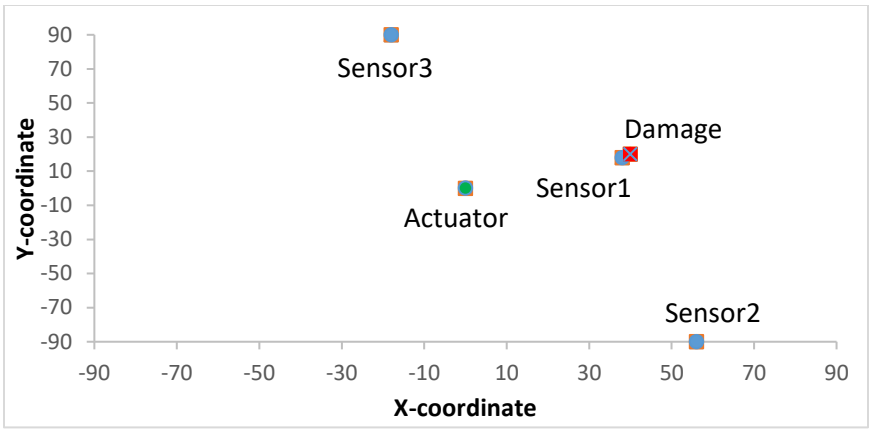

Figure 5-11. Optimal sensor placement for Actuator= (0, 0) and damage= (40, 20)

Example 2. Mean of the Damage location $= \binom{40}{20}$, Actuator $= \binom{35}{15}$

In this example, we place the actuator very close to the damage to see how it would impact the placement of the sensors.

$\boldsymbol{p}_{s1} = \binom{38}{18}$, $\boldsymbol{p}_{s2} = \binom{50}{-52}$, $\boldsymbol{p}_{s3} = \binom{-38}{68}$

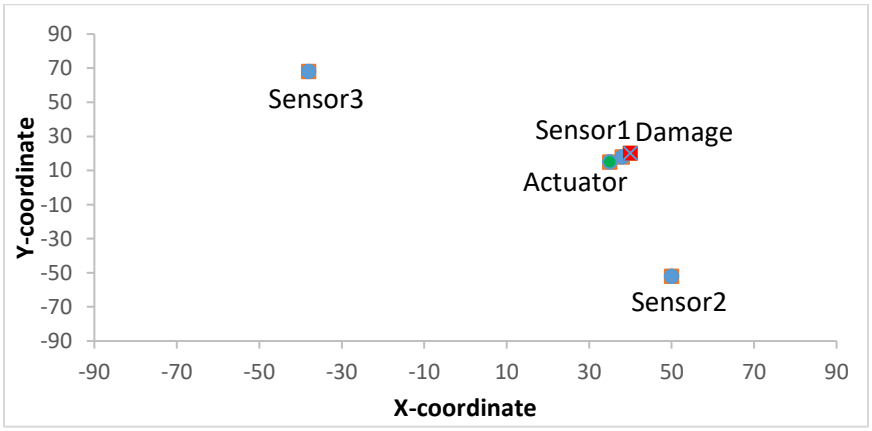

Figure 5-12. Optimal sensor placement for Actuator= (35, 15) and damage= (40, 20)

Example 3. Mean of the Damage location $= \binom{40}{20}$, Actuator $= \binom{-70}{-85}$.

In this example, we move the actuator farther away from the damage. As it can be seen in Figure 5-13, the optimal sensor locations have been moved to:

$\boldsymbol{p}_{s1} = \binom{38}{18}$, $\boldsymbol{p}_{s2} = \binom{90}{-62}$, $\boldsymbol{p}_{s3} = \binom{-66}{90}$

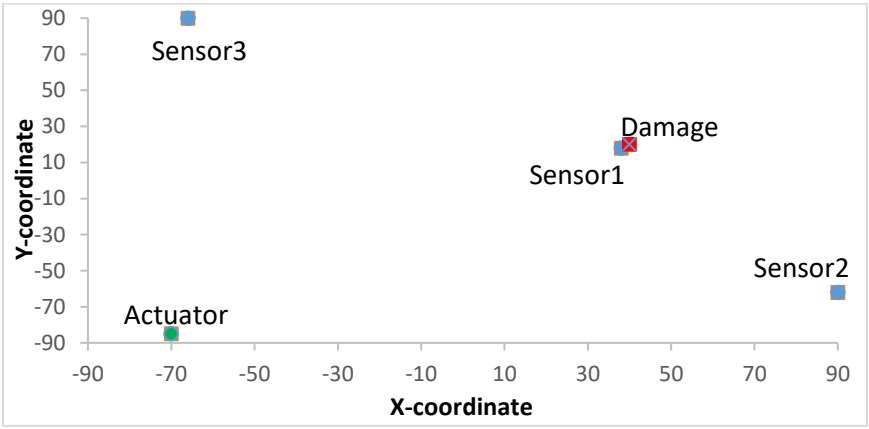

Figure 5-13. Optimal sensor placement for Actuator= (-70, -85) and damage= (40, 20)

Example 4. Mean of the Damage location $= \binom{-40}{-20}$, Actuator $= \binom{-75}{-85}$.

Finally, we move the damage location to the negative side of coordinate, and observe the effect on the movement of the sensors.

$\boldsymbol{p}_{s1} = \binom{-42}{-22}$, $\boldsymbol{p}_{s2} = \binom{62}{-90}$, $\boldsymbol{p}_{s3} = \binom{-88}{-6}$

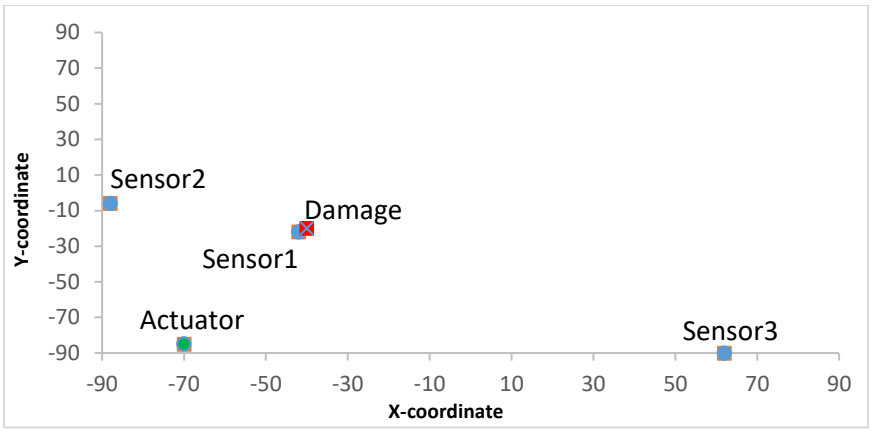

Figure 5-14. Optimal sensor placement for Actuator= (-70, -85) and damage= (-40, -20)

We can see that the actuator has a small impact on the sensor placement. When we move the actuator closer or farther away from the damage, the sensors also tend to be placed closer or farther away to the mean of the damage location respectively. This happens due to the fact that the elements of Fisher information matrix are the functions of the distance of actuator and sensors from damage. So, to have the minimum PCRLB, sensors tend to be located closer to the target. One Sensor is always placed close to the target to get the most information from it.

5.6 PCRLB Comparison

In this section, we provide the trace of the PCRLB matrix for different sensor placement solutions with:

mean of the damage location $= \binom{40}{20}$ and actuator $= \binom{0}{0}$.

Table 5-7 shows that the trace of PCRLB of 1.6361 is achieved when the sensors are randomly placed in the plate, following a uniform distribution. The trace of PCRLB is 1.3330 when an

initial guess, reported in Table 5-1, is used to estimate the damage location. When the sensors are optimally placed in the plate, a minimum trace of PCRLB, 1.1797, is achieved.

Table 5-7. PCRLB Comparison for different sensor locations

Sensor Locations	PCRLB	Trace of PCRLB
Random placement	$\begin{bmatrix} 0.5203 & -0.4862 \\ -0.4862 & 1.1158 \end{bmatrix}$	1.6361
Placement used in Table 5-1	$\begin{bmatrix} 0.4612 & -0.3203 \\ -0.3203 & 0.8718 \end{bmatrix}$	1.3330
Optimal placement	$\begin{bmatrix} 0.4303 & -0.1668 \\ -0.1668 & 0.7494 \end{bmatrix}$	1.1797

5.7 Uncertainty Ellipses

In this section, we want to show the uncertainty ellipses of the prior, the measurement, and the posterior.

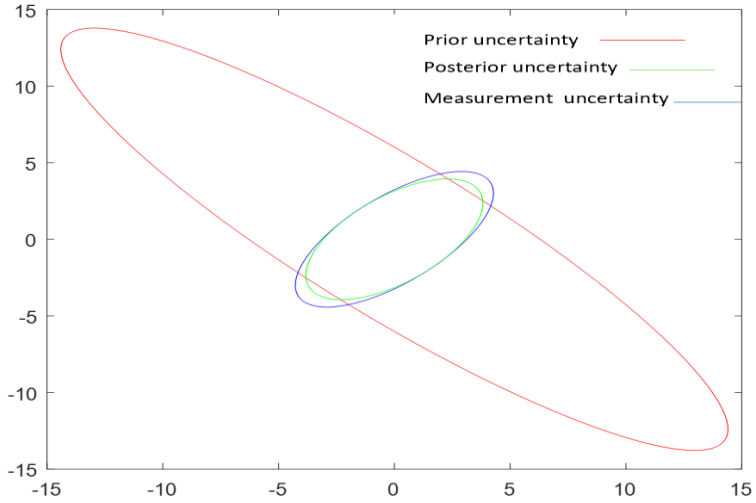

Figure 5-15. Posterior, measurement, and prior uncertainty for $\sigma_\varepsilon^2 = 10^{-12}$

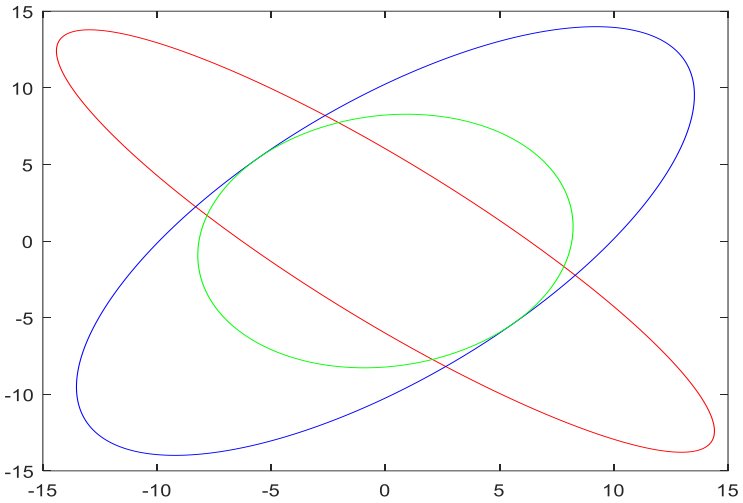

Figure 5-16. Posterior, measurement, and prior uncertainty for $\sigma_{\varepsilon}^{2} = 10^{-11}$

In Figures 5-15 and 5-16, we compare the uncertainty for different variance noises. As it can be seen, in both figures, the posterior uncertainty is smaller than the measurement uncertainty which means more accurate estimation is achieved. Also, with the larger noise, less measurement information will be achieved, so the uncertainty for the updated information will be increased.

6 Chapter 6 Conclusion

The Bayesian model was shown to be successful for a large number of applications with increased estimation accuracy. One of the main contributions of this thesis is to compute the Bayesian-FIM and introduce the PCRLB for Bayesian estimation problems.

In this thesis, we presented a Bayesian estimation approach for localizing a damage in a square plate by using multiple sensors, considering the uncertainties from modeling and measurements. After measuring the calculated ToF of waves in each actuator–sensor path, the Bayesian approach estimates the damage location. A MC algorithm for estimating the posterior distribution is proposed in this thesis. The target location estimate has a very low error.

We presented an evaluation approach for Bayesian-FIM or PCRLB including an approximation. For the nonlinear systems, it is not realistic to have the analytical closed-form for the PCRLB. Hence, we proposed Monte Carlo approximation to provide a proper numerical evaluation solution. So, the PCRLB is calculated through this approximation. Furthermore, we compared it with the mean squared error for different measurement noises to illustrate that the PCRLB indeed provides a lower bound on the MSE.

The PCRLB has different usages in applications. One of the important fields is sensor management in sensor networks. Selecting a subset of sensors that have the most information can improve the estimation performance, while at the same time reduce the requirement for communication and the energy needed by sensors for local computation and communication.

In this thesis, the derived PCRLB was used for sensor placement for target localization. The positions of multiple sensors were optimized, by minimizing the trace of the PCRLB matrix.

The proposed algorithm applied here, select the sensor positions with the minimum cost.

Simulation results demonstrated the significantly improved localization performance by optimally placing the sensors.

For the future work, PCRLB can be applied in recursive mobile sensor placement to improve the estimation results. Also, we can compare different criteria and optimization algorithms for sensor placement.

References

[1] Olfati-Saber R, Fax JA, Murray RM. Consensus and Cooperation in Networked Multi-Agent Systems. Proceedings of the IEEE 2007;95(1):215-33.

[2] Akyildiz IF, Su W, Sankarasubramaniam Y, Cayirci E. A survey on sensor networks. IEEE Communications magazine 2002;40(8):102-14.

[3] Farrar CR, Worden K. An introduction to structural health monitoring. Philosophical Transactions of the Royal Society A: Mathematical, Physical and Engineering Sciences 2006;365(1851):303-15.

[4] Giurgiutiu V, Cuc A. Embedded non-destructive evaluation for structural health monitoring, damage detection, and failure prevention. Shock and Vibration Digest 2005;37(2):83.

[5] Memmolo V, Maio L, Boffa ND, Monaco E, Ricci F. Damage detection tomography based on guided waves in composite structures using a distributed sensor network. SPIE; 2015.

[6] Rojas E, Baltazar A, Loh K. Damage detection using the signal entropy of an ultrasonic sensor network. Smart Materials and Structures 2015;24(7):075008.

[7] Mitra M, Gopalakrishnan S. Guided wave based structural health monitoring: A review. Smart Materials and Structures 2016;25(5):053001.

[8] Chong C-Y, Kumar SP. Sensor networks: evolution, opportunities, and challenges. Proceedings of the IEEE 2003;91(8):1247-56.

[9] Farrar CR, Park G, Todd MD. Sensing Network Paradigms for Structural Health Monitoring. In: Mukhopadhyay SC, editor New Developments in Sensing Technology for

Structural Health Monitoring. Berlin, Heidelberg: Springer Berlin Heidelberg; 2011, p. 137-57.

[10] Flynn Eric B, Todd Michael D, Wilcox Paul D, Drinkwater Bruce W, Croxford Anthony J. Maximum-likelihood estimation of damage location in guided-wave structural health monitoring. Proceedings of the Royal Society A: Mathematical, Physical and Engineering Sciences 2011;467(2133):2575-96.

[11] Kudela P, Radzienski M, Ostachowicz W, Yang Z. Structural Health Monitoring system based on a concept of Lamb wave focusing by the piezoelectric array. Mechanical Systems and Signal Processing 2018;108:21-32.

[12] Hameed MS, Li Z, Chen J, Qi J. Lamb-Wave-Based Multistage Damage Detection Method Using an Active PZT Sensor Network for Large Structures. Sensors 2019;19(9):2010.

[13] Qing X, Li W, Wang Y, Sun H. Piezoelectric Transducer-Based Structural Health Monitoring for Aircraft Applications. Sensors 2019;19(3):545.

[14] Yan G. A Bayesian approach for damage localization in plate-like structures using Lamb waves. Smart Materials and Structures 2013;22(3):035012.

[15] Kehlenbach M, Das S. Identifying damage in plates by analyzing Lamb wave propagation characteristics. SPIE; 2002.

[16] Lemistre M, Balageas D. Structural health monitoring system based on diffracted Lamb wave analysis by multiresolution processing. Smart Materials and Structures 2001;10(3):504-11.

[17] Lu Y, Ye L, Su Z. Crack identification in aluminium plates using Lamb wave signals of a PZT sensor network. Smart Materials and Structures 2006;15(3):839-49.

[18] Zhongqing S, Xiaoming W, Li C, Long Y, Zhiping C. On Selection of Data Fusion Schemes for Structural Damage Evaluation. Structural Health Monitoring 2009;8(3):223-41.

[19] Guratzsch RF, Mahadevan S. Structural Health Monitoring Sensor Placement Optimization Under Uncertainty. AIAA Journal 2010;48(7):1281-9.

[20] Zhao S, Chen BM, Lee TH. Optimal sensor placement for target localisation and tracking in 2D and 3D. International Journal of Control 2013;86(10):1687-704.

[21] Van Trees HL. Detection, estimation, and modulation theory, part I: detection, estimation, and linear modulation theory. John Wiley & Sons; 2004.

[22] Bar-Shalom Y, Li XR, Kirubarajan T. Estimation with applications to tracking and navigation: theory algorithms and software. John Wiley & Sons; 2004.

[23] Chen M-H, Shao Q-M, Ibrahim JG. Monte Carlo methods in Bayesian computation. Springer Science & Business Media; 2012.

[24] Smith A. Sequential Monte Carlo methods in practice. Springer Science & Business Media; 2013.

[25] Marshall AW. The use of multi-stage sampling schemes in Monte Carlo computations. RAND CORP SANTA MONICA CALIF; 1954.

[26] Kay SM. Fundamentals of statistical signal processing. Prentice Hall PTR; 1993.

[27] Tichavsky P, Muravchik CH, Nehorai A. Posterior Cramér-Rao bounds for discrete-time nonlinear filtering. IEEE Transactions on signal processing 1998;46(5):1386-96.

[28] Tharmarasa R, Kirubarajan T, Peng J, Lang T. Optimization-based dynamic sensor management for distributed multitarget tracking. IEEE Transactions on Systems, Man, and Cybernetics, Part C (Applications and Reviews) 2009;39(5):534-46.

[29] Hernandez M, Kirubarajan T, Bar-Shalom Y. Multisensor resource deployment using posterior Cramér-Rao bounds. IEEE Transactions on Aerospace and Electronic Systems 2004;40(2):399-416.

[30] Zhao F, Liu J, Liu J, Guibas L, Reich J. Collaborative signal and information processing: an information-directed approach. Proceedings of the IEEE 2003;91(8):1199-209.

[31] Hoffmann GM, Tomlin CJ. Mobile Sensor Network Control Using Mutual Information Methods and Particle Filters. IEEE Transactions on Automatic Control 2010;55(1):32-47.

[32] Williams JL, Fisher JW, Willsky AS. Approximate dynamic programming for communication-constrained sensor network management. IEEE Transactions on signal Processing 2007;55(8):4300-11.

[33] Masazade E, Niu R, Varshney PK, Keskinoz M. Energy Aware Iterative Source Localization for Wireless Sensor Networks. IEEE Transactions on Signal Processing 2010;58(9):4824-35.

[34] Rajagopalan R, Niu R, Mohan CK, Varshney PK, Drozd AL. Sensor placement algorithms for target localization in sensor networks. *2008 IEEE Radar Conference.* 2008:1-6.

[35] Bauso D, Pesenti R. Team theory and person-by-person optimization with binary decisions. Siam Journal on Control and Optimization 2012;50(5):3011-28.

[36] Dhillon SS, Chakrabarty K, Iyengar SS. Sensor placement for grid coverage under imprecise detections. *Proceedings of the Fifth International Conference on Information Fusion. FUSION 2002.(IEEE Cat. No. 02EX5997).* 2. IEEE; 2002:1581-7.